

# Quantum effects in aluminum under magnetic breakdown conditions

V. I. Gostishchev, M. A. Glin'skiĭ, A. A. Drozd, and S. E. Dem'yanov

*Institute of Solid-State and Semiconductor Physics, Academy of Sciences of the Belorussian SSR, Minsk and International Laboratory of Strong Magnetic Fields and Low Temperatures, Wrocław, Poland*

(Submitted 22 September 1977)

Zh. Eksp. Teor. Fiz. 74, 1102-1114 (March 1978)

The transverse thermoelectric power developed by high-purity aluminum single crystals of the [100] and [110] orientations was measured in magnetic fields up to 150 kOe. New oscillations of  $2.37 \times 10^{-7}$  and  $0.259 \times 10^{-7}$  Oe $^{-1}$  periods were observed in fields above 60 and 120 kOe, respectively. The first period was due to multiple coherent scattering of electrons by magnetic breakdown regions in the momentum space. The second period was associated with the presence of an extremal section in the longitudinal direction of an electron tube.

PACS numbers: 72.15.Jf

It has been established in several experimental investigations<sup>[1-6]</sup> that measurements of the thermoelectric power in a magnetic field provide a convenient method for investigating various quantum effects which appear in metals as a result of coherent magnetic breakdown (breakthrough). It is known that under the magnetic breakdown conditions the only important interband transitions are those which occur in the parts of the p space where the distances between the classical trajectories are less than  $\kappa^{1/2}b_0$  ( $\kappa$  is the quasi-classical parameter, defined by  $\kappa = e\hbar H/cb_0^2$ ;  $b_0$  is the typical size of a unit cell in the p space).

Coherent quantum effects are very sensitive to external perturbations. They can be observed only if  $\omega_H \tau_i \gg 1$  and  $\omega_H \tau_d \gg 1$  ( $\omega_H$  is the cyclotron frequency,  $\tau_i$  and  $\tau_d$  are the electron relaxation times for the scattering by impurities and dislocations, respectively). Inhomogeneity of the magnetic field does not destroy the electron-wave coherence if this inhomogeneity does not exceed 10% per 1 cm, which is easy to achieve in experiments. The most difficult to satisfy is the condition  $\omega_H \tau_d \gg 1$ . A dislocation density  $N_d$  of the order of  $10^6$  cm $^{-2}$  is typical of single crystals of the majority of metals. According to Morgun *et al.*,<sup>[7]</sup> the dislocation density in aluminum single crystals with the resistance ratio  $R_{293^\circ\text{K}}/R_{4.2^\circ\text{K}} \sim 27000$  is  $N_d \sim 10^5$  cm $^{-2}$ . At this dislocation density we may observe coherent effects beginning from fields of the order of 10 kOe.

It has been reported<sup>[1-3]</sup> that aluminum exhibits a magnetic breakdown trajectory which penetrates all the reciprocal space at the hole zone sites passing along an electron  $\beta$  orbit as a bridge. The occurrence of a deep minimum in a thermoelectric power peak, observed on rotation of a sample near  $H \parallel [100]$ , and also the quadratic rise of the monotonic part of the magnetoresistance with increasing field along the magnetic breakdown directions,<sup>[2,8]</sup> clearly indicate that a two-dimensional region of open trajectories appears in aluminum as a result of magnetic breakdown.

We shall report the construction of a stereographic projection of a region of magnetic breakdown trajectories of aluminum and discovery, in strong magnetic

fields, of new thermoelectric power oscillations. The fairly detailed information available on the singularities of the constant-energy surface of aluminum and the small number of electron orbits participating in magnetic breakdown make their interpretation relatively simple.

## EXPERIMENTAL METHOD

Our investigation was carried out on aluminum single crystals oriented along the [110] (No. 1) and [100] (Nos. 2 and 3) directions. The precision of the orientation was at least 2-3°. Samples of  $4 \times 4 \times 14$  mm dimensions were cut from a zone-purified aluminum ingot. A disturbed surface layer was removed by etching; after annealing and electropolishing, the quality of the crystals and their orientation were checked by an x-ray method. The residual resistance ratio  $R_{273^\circ\text{K}}/R_{4.2^\circ\text{K}}$  (RRR) of the samples prepared for investigation was 19 500, 19 000, and 20 000. A temperature gradient was created by an electric heater mounted on one of the ends of the sample. The homogeneity of the heat flow was improved by inserting heating elements in a series of through apertures drilled parallel to the end wall. Good thermal contact between the heating elements and the sample was ensured by filling these apertures with a composition characterized by a sufficiently high thermal conductivity at helium temperatures. The thermoelectric power of aluminum was measured relative to lead (of the S-0000 grade); a lead wire 0.3 mm in diameter, insulated from the sample by a thin insulating spacer, was in thermal contact over its whole length and in electrical contact only at one point at the "warm" end.

The assembled sample was wrapped in a large number of layers of thin paper and was then placed in a protective can made of a nonmagnetic material; the "cold" end and all the electrical contacts were immersed in liquid helium. The sample was rotated and inclined by a rotating device built in accordance with the description given by Alekseevskii *et al.*<sup>[9]</sup> The positions of the crystallographic axes of the sample relative to the  $H = \{0, 0, H\}$  field were determined from

the peaks of the angular distribution of the thermoelectric power by smooth variation of the tilt of the sample. When the sample was aligned correctly, the peaks should be maximal and equal. The temperature gradient across the sample was estimated using a Cu-(Au+0.07% Fe) differential thermocouple calibrated in a magnetic field. When a sample was rotated in a magnetic field, there were no changes in the thermocouple readings. Measurements were carried out at average temperatures of the sample 2.4 and 4.8°K in the field of a Bitter solenoid of up to 150 kOe intensity. The inhomogeneity of the field in the working volume did not exceed 0.25% per 1 cm. The thermoelectric power was recorded continuously on a chart; the relative error of these measurements did not exceed 1–2%.

We investigated the topology of the region of magnetic breakdown trajectories. This was done by recording the same thermoelectric power peak in a field of constant intensity varying the angle of tilt  $\theta$  of the longitudinal crystallographic axis of the sample in a plane passing through this axis and the magnetic breakdown direction. The field dependences of the thermoelectric power were recorded along the magnetic breakdown direction in the crystal for a fixed position relative to the field  $H$ . The main difficulty was to ensure a constant orientation of a sample in a varying magnetic field. The high quality of the investigated samples resulted in the generation of considerable Foucault currents, which gave rise to a considerable mechanical torque. The retention of the initial position in the recording of the field dependences was monitored by checking whether the resultant records were reproducible. Deflection by just a few angular minutes altered the nature of the curve. Since such a high precision of positioning of the sample could not be guaranteed in our apparatus, the correctness of the results obtained was checked by recording also the angular dependences of the same thermoelectric power peak for different values of the magnetic field. The control dependences on the field were then plotted point by point.

## RESULTS OF AN INVESTIGATION OF THE PROFILE OF THERMOELECTRIC POWER PEAKS

The profiles of thermoelectric power peaks obtained by rotating a sample through an angle  $\varphi$  in a transverse magnetic field were investigated with the sample inclined at an angle  $\theta$  in a plane passing through its longitudinal crystallographic axis and the magnetic breakdown direction. Since the peak profiles were found to be symmetric relative to the central position ( $\theta=0^\circ$ ), we reproduced in Fig. 1 only the results obtained for one inclination of the sample relative to this position.

It is clear from the reproduced records that the height and width of the thermoelectric power peaks differed considerably in the central position. In the case of the samples oriented along the [100] axis, the width of the peaks at 0.7 of the maximum height was  $\sim 1^\circ$ , whereas for the samples oriented along the [110] axis it was 4–5°. Moreover, in the former case the

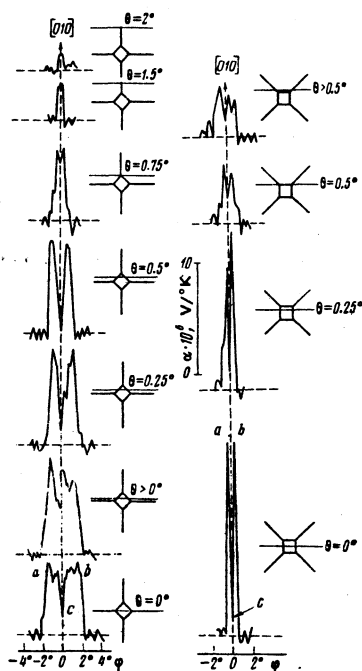


FIG. 1. Records of thermoelectric power peaks obtained by inclining a sample relative to the central position ( $\theta=0$ ) in a plane passing through the longitudinal crystallographic axis and the magnetic breakdown direction. The record on the left was obtained when the sample was oriented along the [110] axis in a field  $H=88.8$  kOe and the right record when the sample was oriented along the [100] axis in a field  $H=94.5$  kOe. The position of the  $H$  scanning line at the moment of record is represented by a thin horizontal line in the stereographic projection of the region of magnetic breakdown trajectories.

peak was split into two by a deep dip, whereas in the latter case the top was almost flat with just two or three shallow minima.

An increase of  $\theta$  from 0 to  $0.25^\circ$  had hardly any influence on the profile of the thermoelectric power peaks exhibited by samples Nos. 2 and 3 (orientation along the [100] axis). The changes appeared only in the range  $\theta \geq 0.5^\circ$ , when the signal became weaker and broader; the deep dip was replaced with a maximum. In this way the top of a peak was found to consist of three maxima and two shallow minima. Further increase in  $\theta$  reduced rapidly the amplitude of the peaks until they became indistinguishable against the noise background ( $0.3 \mu\text{V}$ ).

In the case of sample No. 1 ([110] orientation) an increase in the tilt angle  $\theta$  reduced the peak width. First, the narrowing was accompanied by an increase in the peak height and dip depth. Then, in the range  $\theta \geq 0.5$  there was no further rise of the height, the dip depth decreased, and the peak became bell-shaped at  $\theta=1^\circ$ . Finally, it disappeared in the noise background when the tilt angle reached  $\theta=2.5^\circ$ .

## RESULTS OF AN INVESTIGATION OF THE FIELD DEPENDENCES OF THE THERMOELECTRIC POWER

In recording the field dependences of the thermoelectric power, the sample was set in its central position

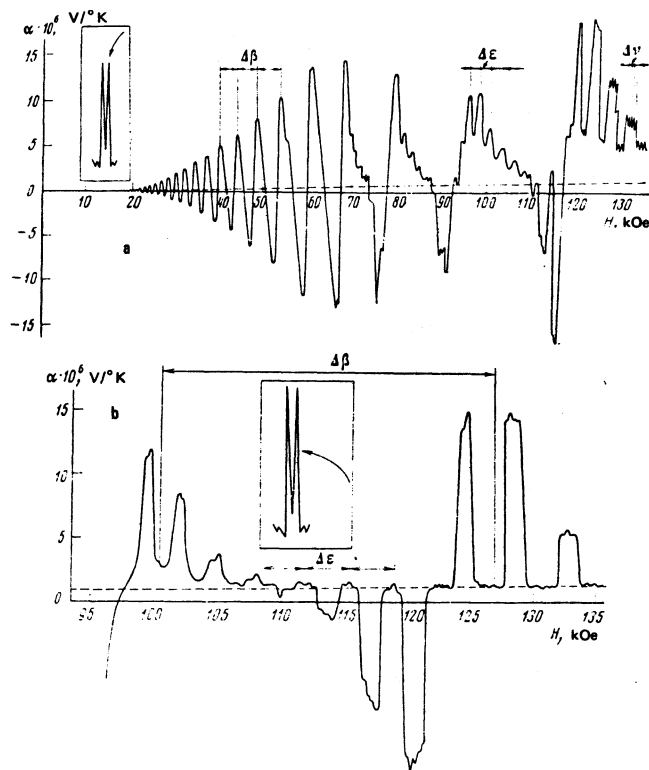


FIG. 2. Oscillations of the thermoelectric power of sample No. 3 (oriented along the [100] axis) in a magnetic field. The insets show the peaks in an angular distribution with arrows identifying the magnetic breakdown trajectory at the moment of record. The records were obtained at  $T = 4.8$  K; in all cases  $\Delta T$  was the same:  $\sim 1$  K.

( $\theta = 0$ ). The investigated point within the region of magnetic breakdown trajectories was selected by rotating the sample in a transverse magnetic field. The field dependences of the thermoelectric power of sample No. 3 are presented in Fig. 2.

The thermoelectric power recorded as a function of  $H$  at the top of the peak in the  $H \parallel [010] \pm 0.5^\circ$  orientation (Fig. 2a) consisted of three periodic components, each of which was a simple harmonic of  $H^{-1}$ . The oscillation periods differed considerably and this made it possible to separate them easily:  $\Delta(1/H) = 21.7 \times 10^{-7}$ ,  $2.37 \times 10^{-7}$ , and  $0.259 \times 10^{-7} \text{ Oe}^{-1}$ . The period of the low-frequency oscillations coincided with the de Haas-van Alphen (dHvA) period for the  $\beta$  orbit, as pointed out earlier.<sup>[1-3]</sup> In the temperature range 2.4–4.8 K the amplitude value of the  $\beta$  oscillations varied exponentially with respect to the reciprocal field (up to  $H \sim 60$  kOe). The oscillations with the period  $2.37 \times 10^{-7} \text{ Oe}^{-1}$  ( $\epsilon$  oscillations) and those with the period  $0.259 \times 10^{-7} \text{ Oe}^{-1}$  ( $\nu$  oscillations) were observed by us for the first time (Table I). The  $\epsilon$  oscillations averaged over the frequency became clearly distinguishable in  $H \sim 65$  kOe but the  $\nu$  oscillations were distinguishable only in  $H \sim 120$  kOe. Their appearance coincided with a reduction in the amplitude of the  $\beta$  oscillations.

At the point corresponding to the middle of the deep minimum the thermoelectric power was practically unaffected by the field; saturation was observed. In the

TABLE I. Periods of oscillations corresponding to extremal sections of the Fermi surface of aluminum in the (100) plane.

Orbit	$\Delta(1/H) \times 10^{-7}, \text{ Oe}^{-1}$		
	Calculation	Experiment	
		dHvA effect	thermoelec. power and elec. resistivity
Second zone			
Large hole $\psi$ orbit	$0.0225$ [10]	—	$2.37^*$
Third zone			
Four-cornered ring orbit	—	$0.115$ [11]	—
ditto, internal	$0.163$ [10]	$0.165$ [12]	—
ditto, external	$0.101$ [10]	—	—
thickening at junctions of two tubes ( $\beta$ orbit)	$21.6$ [10]	$21.74$ [11]; $21.3$ [12]	$21.8$ [8]; $21.7$
along tube	$0.211$ [10]	—	$0.259$

\*Interference period.

case of the “binary” sample (No. 1) the saturation of the thermoelectric power was also retained at the center of the minimum. A slight deviation from the center of this narrow minimum gave rise to a thermoelectric power component, which oscillated with the field. For example, in the  $H \parallel [010] \pm 0.4^\circ$  position the resultant curve already consisted of two periodic components representing the  $\beta$  and  $\nu$  oscillations, and the oscillations with the frequency  $\nu$  had the higher amplitude. The  $\nu$  oscillations were observed most clearly when the temperature of the sample was lowered to 2.4 K and then they appeared in weaker fields. An estimate of the cyclotron mass of the carriers participating in  $\nu$  oscillations yielded the value  $m^*/m = 0.45$ , which was deduced from the temperature dependences.

At a point lying in a steeply falling part of a peak when the field was  $H \parallel [010] \pm 0.8^\circ$  (Fig. 2b) the resultant experimental curve again consisted of two periodic components:  $\beta$  and  $\epsilon$  oscillations. The shape of the curve was now much more complex. It could be regarded as a superposition of two periodic oscillations, in which the oscillations with the average frequency were modulated by slow additional oscillations. Cooling to 2.4 K did not produce any significant change in the amplitude of the  $\epsilon$  oscillations. Rotation of  $H$  about the [010] axis through an angle  $\varphi > 0.8^\circ$  was accompanied by a strong reduction in the amplitude of the  $\beta$  oscillations and complete disappearance of the  $\epsilon$  oscillations. Nevertheless, weak  $\beta$  oscillations with the period  $\Delta(1/H) \sim 20 \times 10^{-7} \text{ Oe}^{-1}$  were observed even when the rotation angle  $\varphi$  was  $45^\circ$ .

All the field dependences of the thermoelectric power obeyed certain general relationships associated with the presence of a nonoscillatory background which was clearly due to the Nernst-Ettingshausen effect: when the field direction was reversed, the sign of this background was also reversed. Moreover, smooth parts of the nonoscillatory curve alternated with jumps. This could be a consequence of the fact that in a strong magnetic field a sample splits into alternate domains with the inductions  $B_1$  and  $B_2$ , where  $B_1 \neq B_2$  (Shoenberg effect).<sup>[14]</sup>

## DISCUSSION OF RESULTS

1. *Stereographic projection.* The dependences of the thermoelectric power on the angle  $\varphi$  in the magnetic breakdown direction (Fig. 1) can be interpreted as follows<sup>[15]</sup>: the points  $a$  and  $b$  correspond to a boundary of a two-dimensional region of open trajectories, which form in aluminum as a result of magnetic breakdown; the point  $c$  corresponds to the center of this region. The dimensions of the region and all its topological features are explained by the stereographic projection shown in Fig. 3. The absence of a deep minimum in the angular distribution of the thermoelectric power in the central position of a sample oriented along the [110] axis may be a consequence of the narrowness of the layer of open trajectories in this direction: in this case, even a small deviation of the longitudinal axis from [110] and the unavoidable inhomogeneity of the magnetic field can give rise to the observed dependence. However, we cannot exclude the possibility of a change in the type of trajectory, i.e., the appearance not only of open but also of closed orbits. A comparison of the experimental results with the stereographic projection (Fig. 1) shows that scanning with  $H$  makes the height of the thermoelectric power peak dependent on the angle  $\theta$ , i.e., on the distance of the scanning line from the symmetry axis of the crystal. When this line passes through the center of the magnetic breakdown region, the peak is greater than in the "whisker intersection" case.

In fields up to 47 kOe intensity the topology of the magnetic breakdown region was investigated using apparatus and samples described by us earlier.<sup>[16]</sup> The results of this investigation yielded the conclusion that, in the investigated range of fields, the region of open magnetic breakdown trajectories is limited to two dimensions.

One should also point out that in effects analogous to the dHvA effect there are oscillations only due to extremal sections. In the case of magnetic breakdown in aluminum the reconstructed regions of open trajectories pass through layers whose width is only a few angular minutes. Clearly, the dimensions of the layer are governed by the width of a belt  $\Delta p_x$  near an extremal  $\beta$  orbit, within which we can ignore the depen-

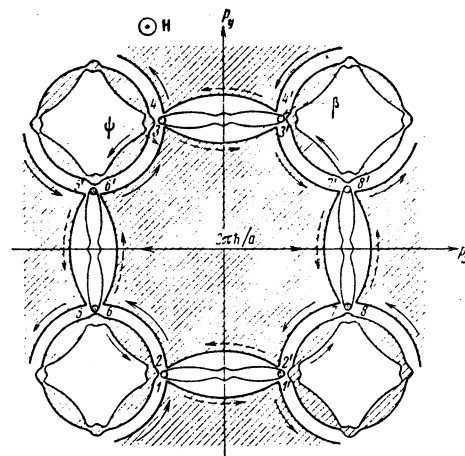


FIG. 4. Central cross section of the Fermi surface of aluminum by the (100) plane. The arrows represent the electron waves: they are continuous for the incident waves and dashed for the reflected waves.

dence of the electron revolution period on  $p_x$  ( $p_x$  is the projection of the electron momentum on  $H$ ).

2. *Oscillations of  $\epsilon$  type.* A physical interpretation of the results obtained can be given by considering the dynamics of magnetic breakdown in a monotonically varying magnetic field. The thermoelectric power oscillations due to magnetic breakdown in our samples become easily distinguishable against the intrinsic noise background beginning from 16.5 kOe (Fig. 2a). An increase in  $H$  up to 65 kOe is accompanied by an exponential rise of the amplitude of the oscillations consisting of a single periodic component. In a field oriented parallel to the [010] axis, carriers precess along the hole  $\psi$  orbits, similar to the orbit defined by the sequence of numbers 2,6,6',3,3',7',7,2',2 in Fig. 4. An increase in  $H$  increases the probability that electrons cross the energy gap. In a field of such direction that carriers in  $\psi$  orbits precess clockwise, the most favorable conditions for magnetic breakdown are provided on parts of the Fermi surface in corners of the hole zone: 3,7',2',6.

In these corners the incident electron wave separates into the transmitted

$$|t\rangle = q \exp(i\varphi_t) \quad (1a)$$

and reflected

$$|r\rangle = (1-q^2)^{1/2} \exp(i\varphi_r), \quad (1b)$$

where  $q^2 = \exp(-H_0/H)$  and  $H_0$  is the breakdown field. A  $\beta$  orbit acts as a bridge through which electrons are transferred from one hole zone to its neighbor. The probability of tunneling of the reflected electron waves to orbits in the neighboring zones in the corners 2,6',3', and 7 is very low because such tunneling disturbs the monotonic variation of the electron velocity. In these corners we find that magnetic breakdown to the zone brings (by the tunnel effect) electrons from the neighboring zones and these replace the lost electrons.

Thus, magnetic breakdown gives rise to open orbits along the crystallographic axes [100] and [001], which

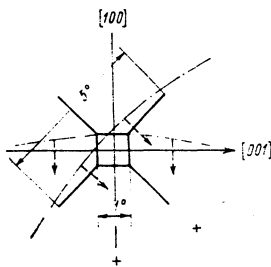


FIG. 3. Stereographic projection of the region of open magnetic breakdown trajectories in a field  $H \approx 90$  kOe. The chain curve shows rotation, the dashed arrows the inclination, and the signs +, - the orientation of the samples whose angular dependences of the thermoelectric power are plotted in Fig. 1.

lie in a plane normal to the field ( $H \parallel [010]$ ). Along each of these directions there are two branches of the open trajectories. For example, along  $p_x$  one branch is  $5'$ ,  $\beta$  orbit,  $6', 7'$ ,  $\beta$  orbit,  $8'$  and the other branch is  $8$ ,  $\beta$  orbit,  $7, 6$ ,  $\beta$  orbit,  $5$ . One-dimensional whisker shape magnetic breakdown trajectories clearly become "incorporated" in the two-dimensional region only beginning from fields of the order of 65–70 kOe.

In determining the nature of the  $\epsilon$  oscillations we must particularly bear in mind that as long as the quasiclassical parameter  $\chi$  is small, the influence of the magnetic breakdown affects only small regions of the  $p$  space whose dimensions are of the order of  $\chi^{1/2}b_0 \sim 10^{-2}b_0$ , which are much smaller than even the dimensions of the  $\beta$  orbit. In the case when the  $\epsilon$  oscillations are due to some new orbit, one may expect a considerable reduction in the amplitude of the  $\beta$  oscillations because the period of the  $\epsilon$  oscillations is almost an order of magnitude less than the  $\beta$  period. In fact, the situation in the case of the  $\epsilon$  component is quite different: the role of the magnetic breakdown not only decreases but even becomes greater. The dependences of the thermoelectric power on  $H$  (see Fig. 2a and particularly Fig. 2b) show that the  $\epsilon$  oscillations are modulated by the  $\beta$  frequency. The modulation coefficient reaches 100%. It is interesting to note that the experimental record in Fig. 2b can be reproduced in practically all its detail by graphical superposition of the  $\epsilon$  and  $\beta$  oscillations. The curve retains only those elements of the  $\epsilon$  component which can be fitted between the envelope of the  $\beta$  curve and zero line. The alternation of the maximal and zero values of the amplitude of the  $\epsilon$  oscillations, observed experimentally, and the very weak temperature dependence are typical of the interference effects.<sup>[17]</sup>

Quantum effects due to the interference between quasiclassical waves scattered in the magnetic breakdown regions in the  $p$  space have been predicted.<sup>[18,19]</sup> In this case we may expect an anomalously strong increase in the magnetic-breakdown thermoelectric power, which may exceed the classical values of this power by a factor  $E_F/kT \sim 10^4-10^5$ . This effect appears only under special conditions when the electron trajectories participating in the magnetic breakdown form, in the  $p$  space, an infinite system of large orbits coupled by small orbits and the average velocity of an electron at right-angles to  $H$  depends periodically on the quasiclassical electron phase on an extremal small orbit. It is known that such special conditions appear in aluminum along crystallographic axes when the conditions are favorable for the magnetic breakdown. Fast oscillations of the electron velocity with energy on a small  $\beta$  orbit are, in fact, responsible for the appearance of the "giant" thermoelectric power. It is shown there that repeated coherent scattering of carriers by the magnetic breakdown regions in  $p$  space should have a considerable effect on the components of the transport coefficients which oscillate in  $H$ . These oscillations may acquire new (interference) periods which are not exhibited by oscillations of any thermodynamic quantities. In addition to a weak temperature dependence, the

TABLE II. Cyclotron masses on extremal sections of the Fermi surface of aluminum in the (100) plane.

Orbit	$m^*/m$		
	Calculation	Experiment	
		dHvA	thermoelectric power
Second zone	1.445 [10]	1.3 [11]	—
Third zone	0.5 [11]	0.8 [11]	—
four-cornered ring	0.495 [10]	—	—
ditto, internal	1.192 [10]	—	—
ditto, external	0.066 [13,10]	0.101 [12]	0.1
thickening at junction of two tubes ( $\beta$ orbit) along tube	0.455 ** [10]	—	0.45

\*\*The calculation is carried out for the [110] direction.

oscillations which are of interference origin are sensitive to deviations of the crystal symmetry axis from  $H$ . This is confirmed very clearly by our experiments. It follows from the field dependences that a change in the angle  $\varphi$  by just  $0.3^\circ$  alters the  $\epsilon$ -oscillation period.

Thus, the appearance of the  $\epsilon$  oscillations under the magnetic breakdown conditions confirms the theoretical predictions<sup>[18,19]</sup> and demonstrates directly the coherence of the magnetic breakdown throughout the  $p$  space, i.e., for small and large electron orbits.

3. *Oscillations of  $\nu$  type.* The area corresponding to the  $\nu$ -oscillation period may represent one of the longitudinal sections of the convex part of an electron tube in the third zone. An estimate of the cyclotron mass of carriers responsible for these oscillations (Table II) confirms this assumption. The appearance of symmetry of the  $\nu$  oscillations relative to the (100) plane corresponds to a symmetric distribution of four-cornered rings in the  $p$  space. In a plane passing through saddle point on such a ring we may have two nearby orbits: one around the convex part of the tube and the other, smaller, around the thickening around the junction of two tubes. The areas corresponding to these orbits are asymmetric relative to the Cartesian axes so that one of them passes through the centers and the other through the saddle point, which corresponds to the condition of appearance of an oscillatory correction in terms of  $H$ . Clearly, the  $\nu$  oscillations are of the quasiclassical type and they should be dominated either by extremal sections or by sections which are tangential to the saddle points. The contribution of the latter can be ignored because it is  $1/\chi^{1/2}$  times less than the contribution of the extremal orbits.

It may seem strange that closed sections make almost the same contribution to the thermoelectric power as the open magnetic breakdown configurations. This can be explained by the presence of a "transverse" thermoelectric power associated with the coefficient  $\alpha_{xy}$  in the generalized tensor equation for the current

$$j_i = \sum_k \left( \alpha_{ik} \frac{\partial T}{\partial x_k} + \sigma_{ik} E_k \right)$$

( $i, k = x, y, z$ ;  $\mathbf{E}$  is the electric field;  $\sigma$  and  $\alpha$  are the tensors representing the electrical conductivity and thermoelectric power, respectively). In the case of an

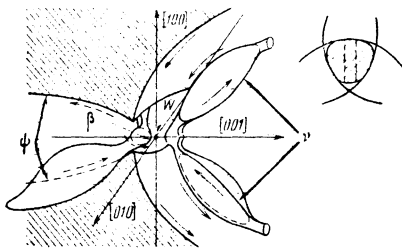


FIG. 5. Model of a part of the Fermi surface of aluminum near the  $W$  symmetry point. The inset shows a transverse cross section of an electron tube in the third zone; the dashed lines are the traces of the planes of an extremal  $\nu$  orbit.

uncompensated metal, such as aluminum, the temperature difference  $\Delta T$  along the  $x$  axis creates a thermoelectric emf

$$U \approx \frac{\alpha_{xx}\sigma_{yy} + \alpha_{yy}\sigma_{xx}}{\sigma_{xx}^2} \Delta T. \quad (2)$$

If  $2\pi^2 kT \lesssim \hbar\omega_H^{(\nu)}$  [ $\omega_H^{(\nu)}$  is the cyclotron frequency of the extremal  $\nu$  orbit], the contribution of the  $\nu$  orbit to  $\alpha_{xy}$  is oscillatory and

$$\alpha_{xy}^{(\nu)} \sim \alpha^{(0)} \frac{E_F}{kT} \frac{\kappa^{1/2}}{\omega_H^{(\nu)} \tau},$$

where  $\alpha^{(0)}$  is the value of  $\alpha_{xy}$  in  $H=0$ , and  $E_F$  is the Fermi energy. On the other hand, the value of  $\alpha_{xx}$  is governed by the contribution of the open (one-dimensional) trajectories; then,

$$\alpha_{xx} \sim \alpha^{(0)} \frac{E_F}{kT} \frac{\delta p}{b_0},$$

where  $\delta p$  is the width of a layer of open magnetic breakdown trajectories (the ratio  $\delta p/b_0 \sim 3 \times 10^{-2}$  for aluminum is comparable with  $\kappa^{1/2} \sim 10^{-2}$ ). Since the number of holes in aluminum is not equal to the number of electrons, it follows that  $\sigma_{xy} \propto \sigma_0/\omega_H \tau$  ( $\sigma_0$  is the conductivity in  $H=0$ ) and  $\sigma_{yy} \propto \sigma_0/(\omega_H \tau)^2$  (the open orbits are retained only along the  $x$  axis). These estimates indicate that the second term  $\alpha_{yy}^{(\nu)} \sigma_{xy}$  in the numerator of Eq. (2) may be comparable (for sufficiently low values of  $T$ ) with the first term  $\alpha_{xx} \sigma_{yy}$ . The location of an extremal  $\nu$  orbit on an electron tube of a four-cornered ring is shown in Fig. 5.

4. *Magnetic breakdown field  $H_0$ .* Dhillon and Schoenberg<sup>[20]</sup> were the first to draw attention to the saturation tendency of the amplitude of the dHvA oscillations of the  $Q$  type in zinc when the field was increased, in contrast to the usual linear field dependence of the dHvA amplitude. This behavior was attributed to the escape of electrons from the closed  $Q$  orbits. In the case of aluminum the experimental points corresponding to the amplitude values of the  $\beta$  oscillations, plotted on a graph in units of  $H^{-1}$ , fitted a nearly exponential curve (Fig. 6). The agreement with the exponential dependence improved when decrease of the field in which the magnetic breakdown was still probable. In fields of 60–65 kOe the experimental curve indicated saturation but its further behavior was unclear because of the complex shape of the oscillatory signal.

By analogy with zinc, we may assume that carriers

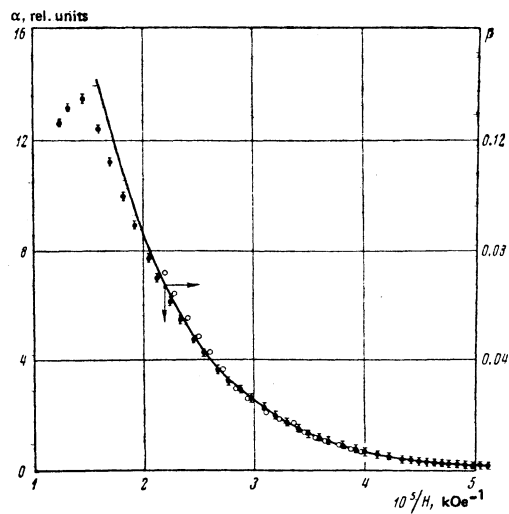


FIG. 6. Dependence of the amplitudes of the  $\beta$  oscillations on  $H^{-1}$ : (●) our results; (○) results of Ref. 6; the continuous curve represents  $\exp(-H_0/H)$  for  $H_0 = 60$  kOe.

are lost within a zone in aluminum because the branches are identical and the motion between them is diametrically opposite. Clearly, the escape is possible at the corners 2, 6', 3', and 7 (Fig. 4) by the tunneling of the reflected-wave carriers to hole surfaces in the neighboring zones. The loss of part of the reflected wave from the  $\psi$  orbit reduces also the transmitted wave, which is confirmed by the experimentally observed deviation of the amplitude of the  $\beta$  oscillations from the exponential law as the field is increased. As pointed out several times before, the  $\beta$  orbit is a "bridge" in the path of the open trajectories which arise as a result of the magnetic breakdown. Since it is assumed that the transverse thermoelectric power is isotropic, independent of collisions with lattice defects, and governed only by the energy spectrum, it follows that a change in the amplitude of the  $\beta$  oscillations is due to a change in connection with the magnetic breakdown. For fixed values of the parameters of the external agency, the change depends on the small parameters of the electron system, governed by the characteristic breakdown field. This field can be determined by comparing the experimental and theoretical values of the magnetic breakdown probability.

The experimental probability of the motion of an electron along a given open trajectory can be determined from the dependence of the thermoelectric power on  $H$ . The problem simplifies because in the range of fields up to 60 kOe a network of magnetic breakdown orbits consists practically of a single trajectory. In the motion along an open trajectory in the  $p$  space in the section 1–4 (Fig. 4) an electron has to overcome an energy barrier twice and the probability of doing that is  $|\langle 1|4 \rangle|^2 = q^4$ . In accordance with Eq. (1), we plotted a large number of theoretical curves for different values of  $H_0$ . The best agreement was obtained for a curve calculated for  $H_0 = 60$  kOe (Fig. 6), which is quite close to the value of  $H_0$  obtained by Morgun *et al.*<sup>[7]</sup> by another method. It should also be pointed out that cooling from 4.8 to 2.4°K does not affect that nature of the ex-

perimental dependence of the amplitude of the  $\beta$  oscillations on  $H^{-1}$ .

The small-amplitude oscillations of the thermoelectric power with a period close to that of the  $\beta$  oscillations, observed in a wide range of angles, are clearly due to small-angle scattering and the resultant transfer of electrons from the second zone to the constant-energy surfaces of the four-cornered rings in the third zone. The periods of these oscillations are clearly governed by the extremal sections of the electron tubes.

It follows that the experimental data obtained in our study support the conclusion that a coherent situation in aluminum single crystals with  $RRR \sim 20\,000$  is realized over the whole p space even in  $H \sim 100$  kOe and  $T \sim 4^\circ\text{K}$ . This is the most important of our results.

The authors are grateful to N. E. Alekseevskii, A. A. Slutskin, and V. I. Nizhankovskii for a useful discussion and valuable comments.

<sup>1</sup>W. Kesternich and C. Papastaikoudis, *Phys. Status Solidi* **64**, K41 (1974).

<sup>2</sup>N. N. Sirota, V. I. Gostishchev, and A. A. Drozd, *Dokl. Akad. Nauk SSSR* **220**, 818 (1975) [*Sov. Phys. Dokl.* **20**, 116 (1975)].

<sup>3</sup>B. J. Thaler and J. Bass, *J. Phys. F* **5**, 1554 (1975); **6**, 2315 (1976); *Phys. Lett. A* **58**, 489 (1976).

<sup>4</sup>V. S. Egorov, *Tezisy dokladov 19-go Vsesoyuznogo soveshchaniya po fizike nizkikh temperatur* (Abstracts of Papers

presented at Nineteenth All-Union Conf. on Physics of Low Temperatures), Minsk, 1976.

<sup>5</sup>N. E. Alekseevskii, K. Kh. Bertel', V. I. Nizhankovskii, M. Glin'skii, and G. Fuks, *Zh. Eksp. Teor. Fiz.* **73**, 700 (1977) [*Sov. Phys. JETP* **46**, 366 (1977)].

<sup>6</sup>W. Kesternich and C. Papastaikoudis, *J. Phys. F* **7**, 837 (1977).

<sup>7</sup>V. N. Morgun, V. I. Khotkevich, N. N. Chebotarev, and V. A. Bondar', *Fiz. Nizk. Temp.* **2**, 1301 (1976) [*Sov. J. Low Temp. Phys.* **2**, 634 (1976)].

<sup>8</sup>R. J. Balkombe and R. A. Parker, *Philos. Mag.* **21**, 533 (1970).

<sup>9</sup>N. E. Alekseevskii, V. I. Nizhankovskii, and K. Kh. Bertel', *Fiz. Met. Metalloved.* **42**, 931 (1976).

<sup>10</sup>N. W. Ashcroft, *Philos. Mag.* **8**, 2055 (1963).

<sup>11</sup>J. R. Anderson and S. S. Lane, *Phys. Rev. B* **2**, 298 (1970).

<sup>12</sup>E. M. Gunnarsen, *Philos. Trans. R. Soc. London Ser. A* **249**, 299 (1957).

<sup>13</sup>C. O. Larson and W. L. Gordon, *Phys. Rev.* **156**, 703 (1967).

<sup>14</sup>D. Shoenberg, *Philos. Trans. R. Soc. London Ser. A* **255**, 85 (1962).

<sup>15</sup>I. M. Lifshitz and M. I. Kaganov, *Usp. Fiz. Nauk* **87**, 389 (1965) [*Sov. Phys. Usp.* **8**, 805 (1966)].

<sup>16</sup>V. I. Gostishchev, A. A. Drozd, and S. E. Dem'yanov, *Tezisy dokladov 19-go Vsesoyuznogo soveshchaniya po fizike nizkikh temperatur* (Abstracts of Papers presented at Nineteenth All-Union Conf. on Physics of Low Temperatures), Minsk, 1976.

<sup>17</sup>R. W. Stark and C. B. Friedberg, *Phys. Rev. Lett.* **26**, 556 (1971).

<sup>18</sup>A. A. Slutskin, *Zh. Eksp. Teor. Fiz.* **58**, 1098 (1970) [*Sov. Phys. JETP* **31**, 589 (1970)].

<sup>19</sup>A. M. Kadigrobov and A. A. Slutskin, *J. Low Temp. Phys.* **6**, 69 (1972).

<sup>20</sup>J. S. Dhillon and D. Shoenberg, *Philos. Trans. R. Soc. London Ser. A* **248**, 1 (1955).

Translated by A. Tybulewicz

## Theory of Mössbauer spectra in the presence of spin-spin relaxation

A. M. Afanas'ev and É. V. Onishchenko

*I. V. Kurchatov Atomic Energy Institute*

(Submitted 28 September 1977)

*Zh. Eksp. Teor. Fiz.* **74**, 1115-1125 (March 1978)

Compared with other mechanisms, spin-spin relaxation substantially complicates the theory of Mössbauer spectra: the relaxation constants become frequency-dependent functions and, in addition, the number of relaxation parameters increases sharply. For systems of cubic symmetry and  $2 \rightarrow 0$  nuclear transitions a method of analysis of the spectra is developed that makes it possible to extract the frequency dependence of the relaxation functions directly from the experimental data for single-crystal samples without invoking any theoretical models. The structure of these functions is analyzed using the method of moments. It is shown that in the case of dipole-dipole interaction the relaxation can be described with good accuracy by one function, the form of which can be established from experimental data obtained on polycrystalline samples.

PACS numbers: 76.80.+y, 76.20.+q

### 1. INTRODUCTION

The theory of Mössbauer resonance spectra that has been developed up to now (see, e.g., Refs. 1-6) is applicable only in those cases when the fluctuations of the magnetic and electric fields giving rise to relaxation of the spin of the electron shell of the Mössbauer

atom are sufficiently rapid, so that the characteristic correlation time  $\tau_c$  of a fluctuation is much shorter than either the relaxation time  $\tau_r$  or the Larmor-precession time  $\tau_L$  of the nuclear spin in the hyperfine magnetic field ( $\tau_L = \hbar/A$ , where  $A$  is the hyperfine-interaction constant).

Both these conditions are fulfilled by a large margin